Acta Crystallographica Section F
Structural Biology Communications
ISSN 2053-230X

Crystallization and preliminary X-ray characterization of the full-length bacteriophytochrome from the plant pathogen *Xanthomonas campestris* pv. *campestris*

Sebastián Klinke,[a] Lisandro H. Otero,[a] Jimena Rinaldi,[a] Santiago Sosa,[a] Beatriz G. Guimarães,[b] William E. Shepard,[b] Fernando A. Goldbaum[a] and Hernán R. Bonomi[a]*

[a]Fundación Instituto Leloir, IIBBA–CONICET, Avenida Patricias Argentinas 435, Buenos Aires, C1405BWE Buenos Aires, Argentina, and [b]Synchrotron SOLEIL, L'Orme des Merisiers, Saint-Aubin BP 48, 91192 Gif-sur-Yvette CEDEX, France

Correspondence e-mail: hbonomi@leloir.org.ar

Received 26 September 2014
Accepted 21 October 2014

Phytochromes give rise to the largest photosensor family known to date. However, they are underrepresented in the Protein Data Bank. Plant, cyanobacterial, fungal and bacterial phytochromes share a canonical architecture consisting of an N-terminal photosensory module (PAS2–GAF–PHY domains) and a C-terminal variable output module. The bacterium *Xanthomonas campestris* pv. *campestris*, a worldwide agricultural pathogen, codes for a single bacteriophytochrome (XccBphP) that has this canonical architecture, bearing a C-terminal PAS9 domain as the output module. Full-length XccBphP was cloned, expressed and purified to homogeneity by nickel–NTA affinity and size-exclusion chromatography and was then crystallized at room temperature bound to its cofactor biliverdin. A complete native X-ray diffraction data set was collected to a maximum resolution of 3.25 Å. The crystals belonged to space group $P4_32_12$, with unit-cell parameters $a = b = 103.94$, $c = 344.57$ Å and a dimer in the asymmetric unit. Refinement is underway after solving the structure by molecular replacement.

1. Introduction

Phytochromes are modular photosensory proteins that detect red and far-red light by photointerconversion between a dark-adapted *Pr* state and a photoactivated *Pfr* state, giving rise to a variety of signalling cascades and photomorphogenic responses. These photosensors, which were first described in plants, are also present in fungi, cyanobacteria and chemotrophic bacteria (Rockwell & Lagarias, 2010; Auldridge & Forest, 2011; Vierstra & Zhang, 2011). Most phytochromes share a canonical domain architecture that consists of an N-terminal photosensory module composed of three domains, PAS2–GAF–PHY, and a C-terminal variable output module. Phytochromes bind bilins (open-chain tetrapyrrole chromophores) as cofactors in their photosensory module. In the specific case of bacteriophytochromes (BphP), the bound bilin corresponds to biliverdin IXα (BV).

Phytochromes are underrepresented in the Protein Data Bank (PDB). Moreover, most of the structures correspond to complete or incomplete photosensory module constructs from bacterial phytochromes. This is probably related to the difficulty in obtaining good diffracting crystals of the full-length proteins, taking into account their multi-domain nature, their considerable size and the intrinsic flexibility between domains. To date, the PDB includes only one phytochrome containing both the complete photosensory module and part of the output module, which corresponds to the *Rhodopseudomonas palustris* CGA009 BphP (PDB entry 4gw9; Bellini & Papiz, 2012*b*). Very recently, single-particle electron microscopy allowed the reconstruction of an entire dimeric BphP containing a histidine kinase as output module, that of the extremophilic bacterium *Deinococcus radiodurans* (Burgie *et al.*, 2014).

The Gram-negative bacterium *Xanthomonas campestris* pv. *campestris* (*Xcc*) is the causal agent of black rot disease and the major bacterial pathogen of cruciferous plants, which include many edible vegetables. *Xcc* codes for a single bacteriophytochrome (XccBphP) that bears a canonical PAS2–GAF–PHY photosensory module linked C-terminally to a PAS9 domain as the output module. As commonly

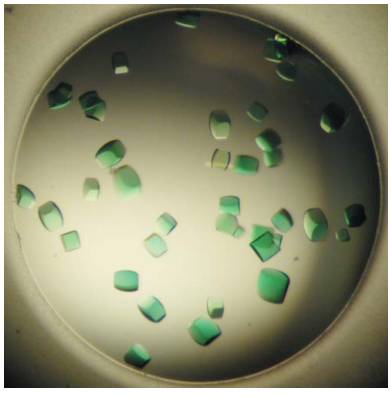

Table 1
Macromolecule-production information.

Source organism	*X. campestris* pv. *campestris* (strain 8004)
DNA source	Genomic
Forward primer (*Nde*I site + His_6 tag)	ATCATATG*CACCATCACCATCACCAT*AGCACTGCAACCAACC-AGCACTGCAACCAACCCGTTG
Reverse primer (*Bam*HI site)	TAGGATCCTTATTCCGGATCGCGCAGCTGTAAC
Cloning vector	pET-24a
Expression vector	pET-24a
Expression host	*E. coli* BL21(DE3)pLysS
Complete amino-acid sequence of the construct produced	MHHHHHHSTATNPLDLDVCAREPIHIPGLIQPYGVLLVIDPA-DGRIVQASTTAADLLGVPMAALLGMPYTQVLTLPEAQPFA-VDDQPQHLMHAEVRFPQRATPPASAWVAAWHLYPQQWLVE-MEPRDARLLDVTLREAMPLLRSVERDPGIAEAAVRVAKGL-RSLIGFDRVMIYRFDEEWNGDIIAEARKPELEAYLGLHYP-ASDIPAQARALYLRNRVRQIADVGYQPSPIQPTVHPQLGT-PVDLSDVSLRSVSPVHLEYLANMGVTATLVASIVVNDALW-GLISCHHYSPHFTNHAMRDVTDAVARTLAGRIGALQAVAR-ARLESVLLTVREKLITDFNDAEHMTVELLDDMAPDLMDVV-DADGVAIFHGNDISRHGTTPDVAALRRIRDHIESEHHEAL-REDAVGALHVDAIGEVFPELADLAPLAAGFIFVPLMPQSR-SALLWTRREQIQQIKWAGNPQLAKLEDIPNSRLSPRKSFD-LWQQTVRGRARRWSPLHLESARSLRVLIELMERKRFQQDF-TLLEASLSRLRDGVAIIERGTANAAHRLLFVNTAFADVCG-SDVAELIGRELQTLYASDAPRANVELLQDALRNGRAAYVT-LPLQVSDGAPVYRQFHLEPLPSPSGVTAHWLLQLRDPE

observed for this family of proteins (Rockwell & Lagarias, 2006), XccBphP forms a dimer in solution (2 × 70.3 kDa; Bonomi *et al.*, unpublished results). It is worth mentioning that dimer formation in BphP has been suggested to be an important factor in successful crystallization (Bellini & Papiz, 2012*a*). To gain insight into the molecular basis of the light-signalling pathway in *Xcc*, we initiated a structure–function analysis of this protein. Here, we present the crystallization and preliminary X-ray data analysis of full-length XccBphP bound to BV at 3.25 Å resolution. This model will represent the first three-dimensional structure of a bacteriophytochrome containing both a complete photosensory and a complete output module.

2. Materials and methods

2.1. Macromolecule production

The gene coding for XccBphP was cloned by PCR using standard protocols and the materials listed in Table 1. The obtained construct, named pET-24a-XccBphP, was checked by DNA sequencing and includes a seven-residue N-terminal cloning artifact (MHHHHHH) followed by the coding region for the complete protein with the exception of its starting methionine (residues 2–634). The construct bears an authentic C-terminus, giving rise to a total of 640 residues. *Escherichia coli* BL21(DE3)pLysS cells transformed with the pET-24a-XccBphP construct were grown overnight in 5 ml LB medium with 50 µg ml^{-1} kanamycin at 37°C with agitation (250 rev min^{-1}) and were then diluted to 500 ml and grown to an absorbance of 0.6 (at 600 nm). At this point, induction was started by the addition of IPTG to a final concentration of 1 m*M*. The bacteria were further cultured for 16 h at 20°C with agitation (250 rev min^{-1}), and were then centrifuged at 9800*g* for 15 min at 4°C. The pellet was resuspended and sonicated in a solution consisting of 20 m*M* sodium phosphate, 0.5 *M* sodium chloride, 20 m*M* imidazole, 1 m*M* PMSF, 1 m*M* DTT pH 7.4 (buffer *A*) and then centrifuged at 160 000*g* in a Beckman Coulter L7-65 ultracentrifuge (Brea, California, USA) for 60 min at 4°C. The supernatant was filtered through a 0.45 µm membrane and loaded onto a HisTrap HP column (all columns were from GE Healthcare, Little Chalfont, England) in a Gilson FPLC apparatus (Luton, England). Elution was performed with a linear gradient of buffer *B* consisting of 20 m*M* sodium phosphate, 0.5 *M* sodium chloride, 0.5 *M* imidazole, 1 m*M* PMSF, 1 m*M* DTT pH 7.4. A major peak was observed at around 25% buffer *B* (Supplementary Fig. S1*a*[1]). The appropriate protein fractions were pooled and incubated for 1 h at room temperature with a threefold molar excess of the green cofactor biliverdin (Sigma–Aldrich, St Louis, Missouri, USA), taking into account that the binding stoichiometry corresponds to one molecule of ligand per protein chain. The resulting mixture was further purified by size-exclusion chromatography on a Superdex 200 16/60 column with isocratic elution in 50 m*M* Tris supplemented with 0.25 *M* sodium chloride pH 7.7. In this case, a major peak was observed at around 80 ml (Supplementary Figs. S1*b* and S2). The final protein fractions were then concentrated to 20 mg ml^{-1} by centrifugation in Amicon Ultra-4 devices (Millipore, Billerica, Massachusetts, USA) and simultaneously exchanged into crystallization buffer (Table 2). The protein was stored at −70°C. The quality of the final preparation was checked by SDS–PAGE (Fig. 1) and UV–Vis spectrophotometry (Supplementary Fig. S3). The protein concentration was estimated using the calculated molar extinction coefficient at λ = 280 nm provided by the ExPASy *ProtParam* tool based on the polypeptide sequence (ε = 148 740 M^{-1} cm^{-1}; Gasteiger *et al.*, 2005), subtracting the contribution from the biliverdin cofactor.

Table 2
Crystallization.

Method	Vapour diffusion, hanging drop
Plate type	Hampton Research VDX (24-well)
Temperature (°C)	21
Light condition	Experiment performed in the dark
Protein concentration (mg ml^{-1})	11
Buffer composition of protein solution	10 m*M* Tris, 25 m*M* sodium chloride pH 7.6
Composition of reservoir solution	12%(*w*/*v*) PEG 4000, 0.1 *M* Tris, 0.2 *M* sodium acetate pH 8.3
Volume and ratio of drop	2 µl, 1:1
Volume of reservoir (µl)	500
Crystallization time (harvesting of the best crystals)	3 weeks
Maximum crystal dimensions (mm)	0.5 × 0.3 × 0.2
Cryoprotectant solution	Mother liquor supplemented with 25%(*w*/*v*) PEG 400

2.2. Crystallization

Initial crystallization trials were performed in 96-well sitting-drop vapour-diffusion Greiner 609120 plates (Monroe, North Carolina, USA) using a Honeybee 963 robot (Digilab, Marlborough, Massachusetts, USA) and the following crystallization kits: Jena Bioscience JBScreen Classic (Jena, Germany) and Hampton Research Crystal Screen, Crystal Screen 2, PEG/Ion, PEG/Ion 2, PEGRx and PEGRx 2 (Aliso Viejo, California, USA). After 5 d of equilibration at room temperature in the dark, eight conditions showed promising hits consisting of tiny green cubes. Some of these conditions were optimized manually with success, and the best diffracting crystals (Fig. 2) were eventually obtained as indicated in Table 2. Samples were cryoprotected and then cooled in liquid nitrogen in Hampton Research loops prior to data collection, with minimal exposure to ambient and microscope light during these steps.

2.3. Data collection and processing

Crystals were tested in-house for diffraction on a Bruker D8 QUEST microfocus diffractometer (Karlsruhe, Germany), and the best data set was collected at the PROXIMA 1 protein crystal-

[1] Supporting information has been deposited in the IUCr electronic archive (Reference: FT5053).

Table 3
Data collection and processing.

Values in parentheses are for the outer shell.

Diffraction source	PROXIMA 1, SOLEIL
Wavelength (Å)	0.97857
Temperature (°C)	−173
Detector	PILATUS 6M
No. of crystals used	1
Crystal-to-detector distance (mm)	577.75
Rotation range per image (°)	0.2
Total rotation range (°)	120
Exposure time per image (s)	0.2
Space group†	$P4_32_12$
a, b, c (Å)	103.94, 103.94, 344.57
α, β, γ (°)	90, 90, 90
No. of chains per asymmetric unit	2
Solvent content (%)	62
Mosaicity (°)	0.09
Resolution range (Å)	47.35–3.25
Total No. of reflections	216820
No. of unique reflections	30865
Completeness (%)	99.9 (100.0)
Multiplicity	7.0 (7.5)
$\langle I/\sigma(I)\rangle$	19.6 (2.4)
R_{meas}	0.116 (1.488)
Overall B factor from Wilson plot (Å^2)	94

† The correct hand was determined during the molecular-replacement search as mentioned in §3.

lography beamline at the SOLEIL synchrotron (France). Fig. 3 shows a particular diffraction pattern from this data set obtained with a PILATUS 6M detector (Dectris, Baden, Switzerland). X-ray diffraction data were processed with *XDS* (Kabsch, 2010) using the graphical user interface *XDSGUI*. A total of 5% of the recorded reflections were flagged for cross-validation. Details of data-collection parameters and processing statistics are shown in Table 3.

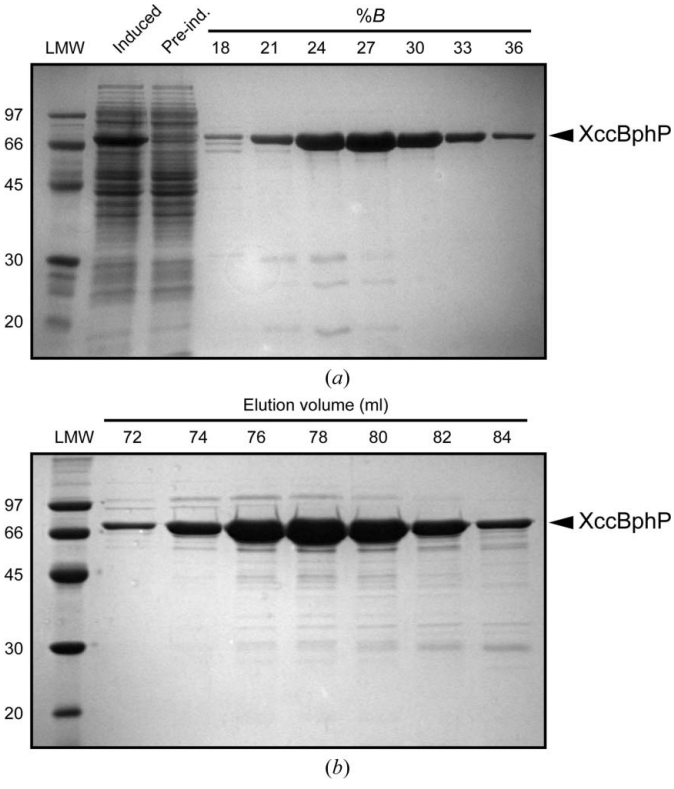

Figure 1
SDS–PAGE gels (15%, Coomassie Blue-stained) for the most relevant stages of the purification process. Standard MW markers are included in the first lanes (LMW) and are labelled in kDa. (*a*) Induction and affinity chromatography step, with selected fractions from 24% to 30% buffer *B*. (*b*) Gel-filtration step, with selected fractions from 77 to 82 ml. The final sample has 95% minimum purity.

3. Results and discussion

XccBphP could be successfully expressed, with an approximate yield of 10 mg per litre of bacterial culture at the end of the purification process. The location of the major protein band in the SDS–PAGE gels (Fig. 1) is in good agreement with the 71 kDa molecular weight calculated from the construct sequence. Minor contaminating bands were still present after the gel-filtration step (Fig. 1*b*), but these impurities did not preclude crystallization of the protein.

Interestingly, the robot screening produced preliminary samples in several conditions buffered at high pH 8.5–9.0, always with the same crystalline habit as shown in Fig. 2. X-ray tests on optimized crystals displayed high variability in their diffraction quality, with most of them showing a poor signal both in-house and at the synchrotron (5 Å resolution or worse, with bad spots). Our experience with XccBphP indicates that working with fresh crystals (cooled in liquid nitrogen long before they reached their maximum size) resulted in better diffraction quality. The best crystal diffracted X-rays to 3.25 Å resolution (Fig. 3) and a complete data set was collected as described in Table 3. Data scaling suggested $P4_12_12$ or $P4_32_12$ as possible space groups.

Solvent-content analysis (Matthews, 1968) is compatible with the following situations: (i) two molecules in the asymmetric unit, with V_M = 3.27 Å^3 Da^{-1} and 62% solvent, and (ii) three molecules in the asymmetric unit, with V_M = 2.18 Å^3 Da^{-1} and 44% solvent. Before any phasing attempts, simply taking into account that XccBphP is a dimer, the first situation appeared to be the correct one. The high solvent content, together with the expected flexibility in this multi-domain protein, might justify the moderate resolution observed and the difficulty in obtaining good diffraction from the crystal samples.

Phasing was achieved by molecular replacement using *Phaser* (McCoy *et al.*, 2007) from the *CCP*4 suite (Winn *et al.*, 2011). For this purpose, the atomic coordinates of the bacteriophytochrome from *Rhodopseudomonas palustris* (Bellini & Papiz, 2012*b*) were used as a search model (PDB entry 4gw9; 28% sequence identity for 613

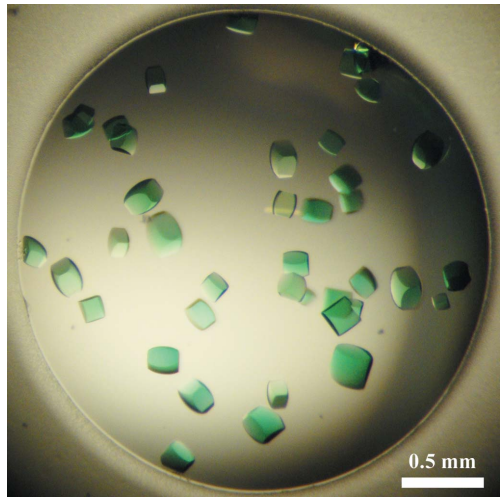

Figure 2
XccBphP crystals. The number of crystals and their final size were highly variable amongst drops during the optimization step.

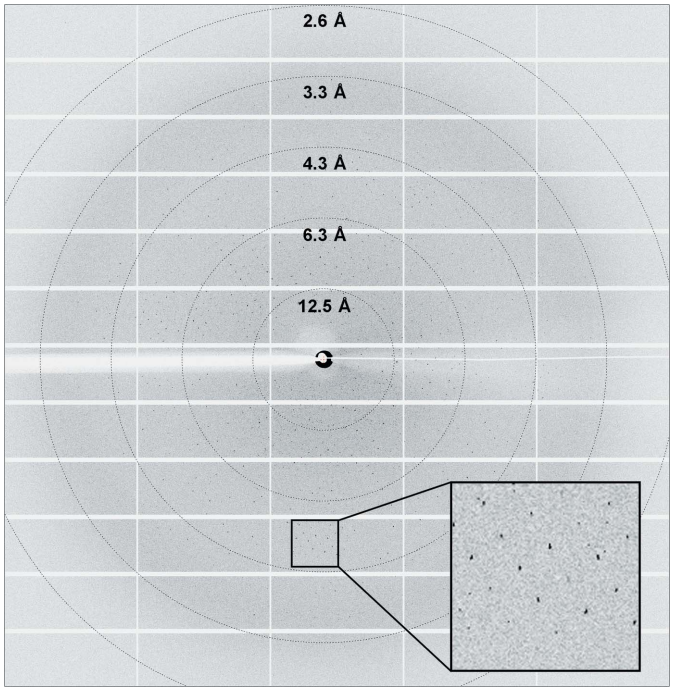

Figure 3
Diffraction pattern. Resolution rings are indicated, and an inset is presented for easier visualization of the spots.

aligned residues). The statistics from *Phaser* included a translation-function *Z*-score of 6.6 and an LLG after refinement of 50. The molecular-replacement step allowed us to confirm both the presence of a dimer in the asymmetric unit and $P4_32_12$ as the space group. Model building and refinement are currently underway, with promising preliminary results (Supplementary Fig. S4).

To summarize, XccBphP, being the first full-length bacteriophytochrome with known three-dimensional structure that includes a complete C-terminal output domain, will provide valuable information about the signal transduction mechanism in this family of photosensory proteins, and might help in understanding the role of light in the pathogenicity of *X. campestris*.

This work was funded by the Argentinian Agency for Scientific and Technological Development (ANPCyT), the Argentinian Ministry of Science (MINCyT) and the Argentinian Research Council (CONICET). We are grateful to the PROXIMA 1 and PROXIMA 2 beamlines at the SOLEIL synchrotron, France, for access to their X-ray facilities.

References

Auldridge, M. E. & Forest, K. T. (2011). *Crit. Rev. Biochem. Mol. Biol.* **46**, 67–88.
Bellini, D. & Papiz, M. Z. (2012*a*). *Acta Cryst.* D**68**, 1058–1066.
Bellini, D. & Papiz, M. Z. (2012*b*). *Structure*, **20**, 1436–1446.
Burgie, E. S., Wang, T., Bussell, A. N., Walker, J. M., Li, H. & Vierstra, R. D. (2014). *J. Biol. Chem.* **289**, 24573–24587.
Gasteiger, E., Hoogland, C., Gattiker, A., Duvaud, S., Wilkins, M. R., Appel, R. D. & Bairoch, A. (2005). *The Proteomics Protocols Handbook*, edited by J. M. Walker, pp. 571–607. Totowa: Humana Press.
Kabsch, W. (2010). *Acta Cryst.* D**66**, 125–132.
Matthews, B. W. (1968). *J. Mol. Biol.* **33**, 491–497.
McCoy, A. J., Grosse-Kunstleve, R. W., Adams, P. D., Winn, M. D., Storoni, L. C. & Read, R. J. (2007). *J. Appl. Cryst.* **40**, 658–674.
Rockwell, N. C. & Lagarias, J. C. (2006). *Plant Cell*, **18**, 4–14.
Rockwell, N. C. & Lagarias, J. C. (2010). *ChemPhysChem*, **11**, 1172–1180.
Vierstra, R. D. & Zhang, J. (2011). *Trends Plant Sci.* **16**, 417–426.
Winn, M. D. *et al.* (2011). *Acta Cryst.* D**67**, 235–242.